Accepted Manuscript

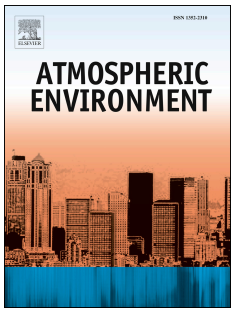

Assessment of NO_X and O_3 forecasting performances in the U.S. National Air Quality Forecasting Capability before and after the 2012 major emissions updates

Li Pan, Daniel Tong, Pius Lee, HyunCheol Kim, Tianfeng Chai

PII: S1352-2310(14)00466-X

DOI: 10.1016/j.atmosenv.2014.06.020

Reference: AEA 13044

To appear in: *Atmospheric Environment*

Received Date: 21 March 2014

Revised Date: 5 June 2014

Accepted Date: 7 June 2014

Please cite this article as: Pan, L., Tong, D., Lee, P., Kim, H., Chai, T., Assessment of NO_X and O_3 forecasting performances in the U.S. National Air Quality Forecasting Capability before and after the 2012 major emissions updates, *Atmospheric Environment* (2014), doi: 10.1016/j.atmosenv.2014.06.020.

Highlights

- NOx emissions were reduced.
- Reduction of NOx emissions improves NOx nighttime prediction.
- Daytime NOx prediction remains a problem.
- Ozone positive bias was reduced after NOx emissions reduction.

Assessment of NO_x and O_3 forecasting performances in the U.S. National Air Quality Forecasting Capability before and after the 2012 major emissions updates

Li Pan[1, 2,*], Daniel Tong[1], Pius Lee[1], HyunCheol Kim[1, 2] and Tianfeng Chai[1, 2]

Affiliations:

[1]: NOAA/OAR/ARL, College Park, MD 20740

[2]: NOAA/Air Resources Laboratory and Cooperative Institute for Climate and Satellites, University of Maryland, College Park

*: Corresponding author: phone: 301-683-1392; email: Li.Pan@noaa.gov

Abstract

In this study, we address outdated emissions inventory problems in air quality forecasting systems. The National Emissions Inventory for NO_x from area and mobile sources is projected from 2005 to 2012 and NO_x from point sources is projected from 2010 to 2012, in which we find that NO_x emissions from area, mobile and point sources reduce by 8.1%, 37.8% and 4.1%, respectively. The majority of the NO_x emissions reduction occurs in megacities over the CONtiguous U.S. (CONUS), in which the spatial distribution pattern is generally supported by the NO_2 column result retrieved from the GOME-2 satellite data. The CMAQ-predicted NO_x and O_3 concentrations using updated NO_x emissions were then compared to Air Quality System (AQS) ground observations in order to evaluate the updated NO_x emissions inventory. The comparison showed an improvement in NO_x and O_3 predictions over the CONUS. The NO_x bias, in July 2011, for urban, suburban and rural land-use types was reduced by 2.34 ppb, 2.09 ppb and 0.57 ppb, respectively. Meanwhile, the O_3 bias is reduced by 0.92 ppb, 1.26 ppb and 1.87 ppb, respectively. However, problems remain in CMAQ for NO_x and O_3 simulations despite undertaking this emissions adjustment. For example, the O_3 overestimation in CMAQ during the daytime over the CONUS decreases when the NO_x underestimation increases, suggesting that in addition to the NO_x emissions inventory, further study of VOC emissions, NO_x chemical and physical mechanisms as well as meteorology parameters in the NAQFC is necessary.

Keywords, NO_x, O_3, CMAQ, Emissions Projection, NAQFC

Introduction

The U.S. National Air Quality Forecasting Capability (NAQFC) addresses public health concerns caused by air pollution. It comprises of two separate numerical predictions (operation and experiment) covering all 50 states of the nation both with 48-hour forecasting. The operational forecast product that consists of surface ozone (O_3) concentrations is available to the public through unrestricted websites and portals. In addition, the experimental forecast product that consists of both O_3 and particulate matter (PM) concentrations is made available to a selected group of local and state AQ forecasters through restricted websites and portals. The experimental forecast is likely to be more advanced in modeling numeric and science yet less reliable in timeliness and availability. In practice both these products are used by local air quality forecasters to issue warnings when potentially harmful air pollution episodes are predicted (Eder et al. 2006; Eder et al. 2009; Gorline and Lee 2009; Kang et al. 2010; Chai et al. 2013).

The NAQFC is a physical modeling system that couples the Weather Research and Forecasting Non-hydrostatic Mesoscale Model (WRF-NMM) (Janjic 2003) and the Community Multiscale Air Quality (CMAQ) (Byun and Schere 2006) regional chemical transport model. CMAQ itself couples the North American Mesoscale (NAM) meteorological model based on WRF-NMM with Arakawa B-grid staggering. The horizontal grid resolution of both the NAM and the CMAQ models is 12 km. The NAM modeling domain covers approximately one-third of the northern hemisphere centered on North America. The NAQFC CMAQ CONUS domain (Figure 1) is then subdivided into six regions in order to analyze geographically specific forecast performance.

The accuracy of the NAQFC's predictions strongly relies on the accuracy of its projected emissions inputs. The emissions inventory used as basis for these projections is the U.S. Environmental Protection Agency (EPA) 2005 National Emissions Inventory (NEI). In the forecasting mode, emissions projection factors are applied to emissions modeling processes. These factors represent the ratios of emissions changes to be imposed on the inventory levels in order to project them to emissions rates at a future time of interest.

Nitrogen oxides (NO_x = NO + NO_2) are not only an important precursor of troposphere O_3 but also a potential source of aerosol formation. According to the base emissions used in this study, 33.6% of NO_x emissions are from on-road mobile sources, 34.3% are from area sources that include activities associated with industrial, commercial and residential zones and 32.1% are from electric-generating units (EGUs) (Figure 2). Although fuel consumption has continuously increased in recent years, NO_x from vehicle emissions, including on-road and off-road, has been decreasing since 2007 (Russell et al. 2010; McDonald et al. 2012) mainly due to the drastic reduction in NO_x emissions after the enforcement of stricter controls (Bishop and Stedman 2008; Dallmann and Harley 2010). NO_x emissions from power plants have also decreased since the implementation of pollution controls by utilities companies (Frost et al. 2006; Kim et al. 2006). Therefore, the direct application of 2005 NEI NO_x emissions rates to the NAQFC for a target year in the 2010s results in the overestimation of NO_x concentration and consequently introduces systematic errors into O_3 forecasting (Chai, Kim et al. 2013).

In this study, we compared surface NO_x and O_3 concentration changes by using two emissions scenarios subject to an "emissions inventory adjustment" in July 2011. The model's

85 results were then verified by using ground station observations. In particular, we addressed the
86 following five questions through the presented process analysis:

87 a) How do NO_x emissions change after this inventory adjustment?
88 b) Is the NO_x emissions change reasonable and supported by our observations?
89 c) Does CMAQ performance in terms of the NO_x and O_3 prediction improve under
90 such an inventory update?
91 d) What are the remaining problems for NO_x after making the NO_x inventory
92 adjustment?
93 e) How is the NO_x prediction change related to the O_3 prediction change?

94 These answers shed light on the emissions projection processes for surface-level NO_x and
95 O_3 concentration forecasting.

96 ## *Methodology*

97 A NAQFC-β (Lee et al. 2009; Lee et al. 2010) , a research version of NAQFC system
98 with a simulation domain covering the CONUS at 12 km horizontal grid spacing was constructed
99 for this study (Figure 1). This system is similar to the coupled NAM-CMAQ modeling system
100 used in the NAQFC, but CMAQ (version 4.7.1) was used. CMAQ 4.7.1 is a newer version than
101 that currently used in the NAQFC. PREMAQ (Otte et al. 2005), an interface processor that
102 provides the means for data exchange from NAM to CMAQ, was used to generate the CMAQ
103 model-ready meteorological input. This processor remaps the meteorology data from a rotated
104 latitude-longitude map projection on an Arakawa-B staggered grid to a Lambert conformal map
105 projection onto an Arakawa-C staggered grid. Horizontally, PREMAQ subsets and transforms

106 the meteorological fields from NAM so that they are ready to be inputted into CMAQ's CONUS
107 domain. Vertically, PREMAQ interpolates NAM's 60 hybrid (top 18 isobaric levels + 42 sigma-
108 p levels) layers to CMAQ's 22 terrains following sigma-p layers with uneven grid spacing. There
109 are 14 layers below 2 km. The model top is 200 pa. The dry deposition velocities for gas and
110 particulate species were also calculated in PREMAQ.

111 Two treatments were used to prepare the model-ready emissions data. For emissions
112 sources that are independent of meteorological influence, emissions projections were processed
113 as a "pre-simulation generated CMAQ input" by using a tool called SMOKE (Sparse Matrix
114 Operator Kennel Emissions) (Houyoux et al. 2000) in order to account for temporal and
115 holiday/non-holiday variations that are year-specific. On the other hand, for those sources
116 influenced by meteorology, their projected rates were generated by using PREMAQ and the
117 forecasted meteorological fields from the NMM model.

118 The Carbon Bond 2005 chemical mechanism (Yarwood et al. 2005) and AERO5 aerosol
119 module (Carlton et al. 2010) are used in CMAQ 4.7.1 in the NAQFC-β system. Online biogenic
120 emissions (BEI3.13) processing in CMAQ is invoked to synchronize with other related processes
121 in each chemistry time step. The lateral boundary conditions used in the simulation are monthly
122 averaged profiles extracted from the GEOS-Chem (Bey et al. 2001) simulation results.

123 We conducted two model runs based on different NOx emissions scenarios subject to an
124 "inventory adjustment" for July 2011. The base run (referred to as "Base" hereafter) used the
125 2005 NEI for the United States and 2001 Environment Canada (EC) emissions inventories for
126 Canada with no "inventory adjustment". The new run (referred to as "New" hereafter) used the

"adjusted" 2005 NEI by superimposing on it changes from 2005 to 2012 for the U.S. and 2006 Canadian inventories for Canada. The biogenic emissions modeling used in these two cases were identical. The details on the emissions differences in the two scenarios are summarized in Table 1 and discussed in the next section.

The model results for NO_x and O_3 were evaluated by comparing the forecasted surface concentration to the observations of all monitoring measurements within the same grid cell. . Finally, EPA Air Quality System (AQS) data accessed on November 7, 2012 were used for this study (http://www.epa.gov.ttn.airs/airsaqs/detaildata/dosnloadaqsdata.htm).

Results and Discussion

- **NO_x emissions inventory upgrade**

Table 1 highlights the differences in the NO_x emissions projection methodology used in the CMAQ simulation in this study between the Base Case and New Case. For the New Case, the CMAQ simulation was driven by an emissions dataset that had the following four major updates from the Base Case. First, it incorporated new point source measurement data and an energy projection for NO_x. Second, it updated on-road emissions by using the 2005 NEI as a basis and scaled it to 2012. Third, it replaced off-road emissions with projected 2012 emissions data. Lastly, it updated all Canadian emissions sectors with EC 2006 emissions inventories. Area, except off-road, source emissions used the same emissions inventories as in the Base Case. Furthermore, the U.S. off-road emissions in the 2005 NEI were replaced with the 2012 emissions data prepared for the Cross-State Air Pollution Rule (CSAPR) (EPA 2011). In addition, except for California, it used simulation results generated from the National Mobile Inventory Model

148 (NMIM), which utilized the NR05d-Bond-final version of the NONROAD model by using
149 future-year equipment population estimates and control programs for 2012.

150 EPA Office of Transportation and Air Quality 2005 on-road emissions inventories were
151 used to generate mobile emissions over the U.S. The ratios of emissions projections between
152 2005 and 2012 in the CSAPR were employed to scale the 2005 NEI to the forecasting year. The
153 CSAPR projection for mobile sources was derived by MOVES (Motor Vehicle Emissions
154 Simulator) version 2010 and NMIM 2012 estimates (EPA 2011). Aggregated state-level data
155 from the U.S. EPA-released CSAPR data were finally used in the subsequent emissions
156 projection.

157 For the point source emissions, 2005 NEI (version 1.0) data were used as the base year
158 for both EGU and non-EGU point sources in the U.S. NO_x emissions from U.S. EGU sources
159 were upgraded with the most recent biannual 2010 Continuous Emissions Monitoring (CEM)
160 data released in 2010. Further, by using the Annual Energy Outlook from the Department of
161 Energy released in January each year for 2012, we projected, on a regional basis, the EGU
162 emissions to 2012 by using the ratios of 2012 to 2010 emissions (DOE 2012).

163 Anthropogenic emissions in the Canadian territories of the domain were updated by using
164 the 2006 National Air Pollution Inventory provided by EC. All Canadian inventories, including
165 mobile, point and area sources, were then processed by using a similar approach as that of U.S.
166 sources. Spatial surrogates, that are used to spatially distribute province-level emissions into
167 model grid boxes, were also provided by EC.

168 • **NO_x emissions reduction (%)**

169 **1. By source**

170 Table 2 shows that NO_x emissions reduced after the NOx inventory adjustment discussed
171 in the previous section. Mobile, point and area emissions sources show a reduction in NO_x by
172 37.8%, 4.1% and 8.1%, respectively. Meanwhile, the weekday NO_x emissions reduction is
173 usually greater than the weekend NO_x emissions reduction (total NO_x emissions reduced by
174 18.3% on weekdays and by 13.5% at weekends). Moreover, the percentage reductions by source
175 sector are as follows: Area source – 10.5% on weekdays and 3.6% at weekends; Mobile source –
176 37.8% on weekdays and at weekends; and Point source – 4.2% on weekdays and 4.0% at
177 weekends.

178 In the Base Case, the distribution of total NO_x emissions in the CONUS among mobile,
179 area and point sources are fairly evenly distributed (33.6%, 34.3% and 32.1%, respectively;
180 Figure 2). In the New Case, they are 25.2%, 37.9% and 36.9%, thus showing a significant drop
181 in the contribution by mobile sources. In the case of anthropogenic NO_x emissions, mobile
182 sources are increasingly becoming less important in contrary with area and point sources.

183 Up to 92% of the NO_x emissions reduction achieved by the New Case is attributed to the
184 reduction in surface sources (i.e. sources within the first model layer). In terms of the changed
185 distribution between the cases based on the injection height groupings of NO_x emissions, we
186 categorize them by surface sources and elevated sources (i.e. sources above the first model full
187 layer). The first layer contribution of NO_x emissions changed from 70% for the Base Case to
188 65.6% for the New Case. For the monthly total surface level NOx emissions for July 2011, the
189 New Case achieved a drop of 22.2%, largely reductions in emissions from mobile and non-road

(area) sources. This significant change alters the chemical regime and air pollutant composition in surface levels and affects surface O_3 production and the titration dynamics.

2. **By region**

The percentage NO_x emissions reductions in the six predefined regions in the CONUS are shown in Figure 1. A reduction occurs in every region. These are stipulated as follows in descending order of the percentage reduction achieved: Upper Middle 21.0%, Pacific Coast 19.2%, South East 17.4%, North East 16.8%, Rocky Mountains 16.1% and Lower Middle 11.5%. The spatial distribution difference plot, that is the New minus Base in NO_x emissions flux in mole/s/grid, is shown in Figure 3a. The largest NO_x emissions reductions are noted in megacity urban areas such as San Francisco, Los Angeles, Dallas, Houston, Chicago, Detroit and Atlanta, which is consistent with the geographical distribution of the dominant NO_x emissions sources.

- **Emissions inventory changes versus satellite observations**

NO_2 column concentrations within the boundary layer, which can be obtained through satellite observations, were used to constrain the NO_x emissions inventory (Velders et al. 2001; van der A et al. 2006; Lamsal et al. 2008; Stavrakou et al. 2008; Kim et al. 2009; Lamsal et al. 2011). We utilized Global Ozone Monitoring Experiment-2 (GOME-2) (Richter et al. 2011; Valks et al. 2011) tropospheric NO_2 column density data for July 2011, retrieved by the Royal Netherlands Meteorological Institute, available from the European Space Agency's Tropospheric Emissions Monitoring Internet Service (TEMIS; http://www.temis.nl/airpollution/no2.html). TM4NO2A (version 2.3) data were used for GOME-2. The GOME-2 sensor, onboard the

EUMETSAT MetOp-A satellite, conducts nadir measurements at near 9:30 am local time with footprints of 40×80 km^2. The Differential Optical Absorption Spectroscopy technique was used for this product. Details on the NO_2 column retrieval algorithms and error analysis have been described by Boersma et al. (Boersma et al. 2004; Boersma et al. 2007). Data pixels with cloud fractions over 40% or contaminated pixels using quality flags are disregarded. The resolution effect over urban cities (Hilboll et al. 2013) was adjusted by using the conservative downscaling method (Kim 2013).

Figure 3b illustrates the averaged NO_2 column concentration difference plot in relative percentages with CMAQ NO_2 minus GOME-2 NO_2 divided by GOME-2 NO_2 for July 2011. The warm colored hot spots in the plot that correspond to megacities and urban areas demonstrate that NO_2 concentrations in those regions are overpredicted in CMAQ. The spatial distribution is in good agreement with that shown in Figure 3a for the difference plot of NO_x emissions fluxes between New minus Base. However, there are three main differences. First, the negative ratios in rural areas indicate that NO_x emissions are increasing. Second, in the North East regions including New York and Boston, Figure 3b indicates that NO_x emissions are increasing, in contrast to the decreasing NO_x emissions shown in Figure 3a. Finally, Figure 3a misses those hot spots in the South East (Florida area) and Lower Middle (Louisiana) regions shown in Figure 3b, implying that the NO_x emissions decrease in those regions would be greater than our estimates.

- **Model evaluations**

    1. **NO_x**

In the next step, the results of the CMAQ simulation for the New Case were verified against the AQS ground station NO_x and O_3 measurements. In concert, the Base Case were also

233 evaluated in order to quantify whether the NOx emissions adjustment used in the New Case
234 leads to performance improvement in NAQFC-β.

235 Figure 4a shows the monthly averaged NO_x bias (Base minus AQS) based on 295 AQS
236 sites over the CONUS in July 2011. Depending on the regions, the model either overestimates or
237 underestimates the NO_x surface concentrations. CMAQ tends to overestimate the NO_x
238 concentrations in the South East and Upper Middle regions as well as megacity areas such as Los
239 Angeles, Houston and Chicago. On the other hand, CMAQ tends to underestimate the NO_x
240 concentrations in the North East, Rocky Mountains, rural areas of the Pacific Coast and Lower
241 Middle. For the New Case, where there was a significant NO_x emissions reduction, the simulated
242 NO_x concentration differences between New and Base (New minus Base) are shown in Figure
243 4b. This figure shows that NO_x positive biases are reduced as simulated NO_x concentration
244 deceases as a result of the NO_x emissions reduction. Although NO_x biases over the CONUS
245 improve (see Figure 4c), Figure 4c shows that in regions such as North East and Rocky
246 Mountains NO_x predictions worsen, suggesting that the negative NO_x bias increases after an NO_x
247 emissions reduction, namely that in those regions NO_x emissions tend to increase instead of
248 decreasing, which is supported by Figure 3b. For the remaining regions, the NO_x positive biases
249 reduced in the South East and Pacific Coast, while the Upper Middle region changed from
250 positive biases to negative biases, suggesting that the NO_x emissions reduction in this region is
251 more than it should be. Finally, the bias in the Lower Middle region remained the highest after
252 the NO_x emissions reduction, indicating that more NO_x emissions should be reduced.

253 Figure 4d shows the diurnal NO_x variation in the AQS observations and in the CMAQ
254 simulations averaged over the CONUS for July 2011. By comparing the simulation results to the

observation values and sorting the comparison by local hours, CMAQ is found to be capable of capturing the NO_x trend of a high peak in the morning and a low peak in the afternoon. Moreover, CMAQ overestimates NO_x at nighttime and slightly underestimates NO_x in the daytime. In addition, the NOx emissions reduction reduces NO_x bias at night by 26%, indicating that a NO_x prediction improvement occurs at night by using the emissions inventory adjustment. Finally, there is no major change in the NO_x daytime bias between the Base Case and New Case, suggesting that the NO_x ambient concentration during the day is not only emissions related but also reactions related.

2. O_3

Based on 1144 AQS ground measurement sites, we find that the modeled O_3 concentration over the CONUS in the Base Case was overestimated in July 2011, except in southern California and Arizona (Figure 5a). By reducing NO_x emissions, Figure 5b shows a modeled O_3 concentration difference plot between the simulation results for the New Case and Base Case (New minus Base). For most regions, the modeled O_3 concentrations in the New Case decrease, indicating that the O_3 positive bias in NAQFC-β has been reduced. In southern California and Arizona, the NO_x emissions reduction in the New Case leads to an increase in the modeled O_3 concentration, reflecting the fact that those regions are NO_x-saturated (Sillman 1999; Fast et al. 2000; Kleinman et al. 2005). In the New Case scenario, the NAQFC-β-predicted O_3 underestimation in those regions was also reduced. However, the New Case prediction in the Houston area showed an NO_x emissions reduction that resulted in an increased O_3 overestimation, thereby reflecting the local emissions inventory problem, especially for VOC (Murphy and Allen 2005). Over the CONUS (Figure 5c), NAQFC-β-predicted O_3 improved

277 overall after the NOx emissions reduction. In all six predefined regions, the O_3 positive biases
278 were reduced. However, in the South East, Upper Middle and Lower Middle regions, the
279 predicted O_3 biases were still above 6 ppbv on average in July 2011.

280 Figure 5d shows the O_3 diurnal variations based on the AQS observations and model
281 simulations for July 2011. After NO_x emissions had been adjusted downwards in the New Case,
282 the O_3 positive biases decreased, which is mostly shown in the afternoon when the surface O_3
283 concentration is highest during the day, reflecting the finding that the high O_3 concentrations
284 simulated in CMAQ benefit more from an NO_x emissions reduction.

285 **3. NO_x and O_3 biases versus land use**

286 Table 3 summarizes the NO_x and O_3 biases over the CONUS in the two NAQFC-β-
287 simulated cases (Base Case and New Case). These biases are categorized according to three
288 land-use types: urban, suburban and rural. For NO_x, the positive bias declined for all three land-
289 use types. Specifically, NO_x biases reduced more (with respect to the absolute value) in urban
290 and suburban areas than in rural areas, since the NO_x reduction is mostly due to mobile
291 emissions reductions (Table 2). The NO_x bias in suburban areas remains the highest. For O_3, the
292 positive bias also reduced in urban, suburban and rural areas. Further, the O_3 bias in rural areas
293 reduced most, reflecting the fact that O_3 is a secondary pollutant produced downwind of NO_x
294 source regions.

295 • **NOx simulation uncertainties**

296 **1. Emissions inventory**

297 According to the emissions update presented in this study, total area, mobile and point
298 NO_x emissions in the North East and Rocky Mountains areas reduced by 16%. The evaluation of
299 the result in the "New" model (Figure 4c) simulation illustrates that the NO_x prediction in
300 CMAQ for those two regions worsened as the NO_x negative bias increased after reducing the
301 emissions. Therefore, the model sensitivity result suggests a potential need to increase NO_x
302 emissions in those two regions. This finding is consistent with the satellite observations
303 illustrated in Figure 3b, since CMAQ underpredicted the NO_2 column in the North East and
304 Rocky Mountains. From this point of view, for NO_x both the emissions inventory projection
305 method and the satellite emissions factor method (Lamsal, Martin et al. 2011) can be utilized as a
306 useful tool to adjust emissions input used in the forecasting model. However, there is a
307 discrepancy between the satellite observations and emissions inventory adjustment. It is easy to
308 adjust the model emissions input by using factors based on satellite observations and model
309 sensitivity studies, but it is difficult to attribute those factors to the emissions inventory for
310 specific sectors.

311 Xing et al. (Xing et al. 2013) found different trends when examining the NO_x emissions
312 reduction in the NEI and the observed NO_2 concentration reduction over AQS sites in
313 Northeastern U.S. from 2005 to 2010, suggesting that the NO_x reduction in mobile sources in the
314 North East may be overpredicted by 10–20%. For the Rocky Mountains area and western U.S.,
315 the rapid growth in industries that produce gas and oil from tar sands significantly increases the
316 NO_x emissions released from this region. These emissions are underpredicted since they are not
317 comprehensively and accurately described in our current NO_x emissions inventory (Bar-Ilan et

318 al. 2009). Meanwhile, soil NO_x, lightning NO_x and NO_x from biomass burning also contribute to
319 our NO_x emissions uncertainty (Lee et al. 1997).

320 **2. Chemical and physical mechanisms**

321 In Figure 4d, in terms of the NO_x peak concentration in the morning, there is a two-hour
322 time shift between the model and observations. The highest NO_x concentration is simulated at
323 6:00 AM in the model, but it is measured at 8:00 AM am in the observations. Lindhjem et al.
324 (Lindhjem et al. 2012) argued that the temporal profile currently used in mobile sources to
325 disaggregate NO_x daily emissions into hourly emissions may be unsuitable since it is assumed to
326 be constant regardless of roadway type (Marr et al. 2002). In addition to the emissions inventory,
327 meteorological aspects such as the planetary boundary layer (PBL) depth may also play a major
328 role in the NO_x morning peak shift. The evolution of the PBL is a critical parameter that
329 significantly affects the CMAQ prediction for NO_x since it is intensively released from urban
330 areas in rush hours with the concurrent morning transition of the PBL (Lin et al. 2008; Wilczak
331 et al. 2009; Doraiswamy et al. 2010).

332 Figure 4d illustrates that NO_x is overestimated at night in CMAQ even after a reduction
333 in NO_x emissions. Understanding how CMAQ deals with the NO_x chemical removal processes at
334 night may be crucial to this overestimation. At night, NO_x is oxidized by O_3 to produce the
335 nitrate radical NO_3. This then yields dinitrogen pentoxide, N_2O_5, which undergoes a
336 heterogeneous reaction on the surface of aerosol particles with H_2O to form HNO_3, and this
337 accounts for 20–50% of the NO_x loss during the night (Lei et al. 2004). CMAQ parameterizes
338 this removal pathway of the loss of NO_x with large uncertainty (Davis et al. 2008). The other

339 potential pathway to remove NO_x from the atmosphere at night is through the heterogeneous
340 conversion of NO_2 to HONO on the ground surface as well as on aerosol (Finlayson-Pitts et al.
341 2003). This mechanism is also involved in CMAQ and it is believed to be the predominant
342 source of HONO at nighttime, although the process is not yet well understood (Sarwar et al.
343 2008).

344 Keeping in mind that NO_x in the AQS observations may be overestimated in the daytime
345 since NO_y is actually measured (Dunlea et al. 2007), CMAQ underestimates NO_x in the day in
346 the Base Case and, at the same time, the emissions inventory is considered to be adjusted
347 downwards in the New Case. In fact, the reduction of NO_x emissions (New Case) enhances the
348 NO_x underestimation in the CMAQ simulation (Figure 4d). The largest underprediction, up to
349 6.3 ppb averaged in July 2011, is at 8:00 AM local time at urban sites. NO_x is removed from the
350 troposphere mainly through HNO_3 deposition via reactions with OH radical. Previous studies
351 have found that CMAQ overpredicts total nitrate (NO_3^- + HNO_3) in the eastern U.S. (Phillips and
352 Finkelstein 2006; Appel et al. 2010) and that the inaccurate shifting of total nitrate from the
353 particle phase to the gas phase may have led to the overprediction of HNO_3 deposition due to the
354 faster dry deposition rate of HNO_3 (Ensberg et al. 2013). Liu et al. found that a decreasing dry
355 deposition velocity of HNO_3 improves overall CMAQ model performance in terms of NO_3^-
356 concentration (Liu et al. 2011).

357 Further, organic nitrate ($RONO_2$) generated through the NO reaction with the organic
358 peroxy radical (RO_2) is an important NO_x reservoir that has a longer lifetime than NO_x and that
359 can be transferred to remote regions. Moreover, isoprene-derived nitrate treated as NTR in
360 CMAQ constitutes a larger proportion of organic nitrate (Beaver et al. 2012) and its lifetime and

fate are questions that remain to be answered (Browne et al. 2013). In CMAQ, its lifetime is suggested to be roughly 7~10 days compared to the one-day lifetime estimated elsewhere (Perring et al. 2009). Another recent study has found that CMAQ overestimates organic nitrate in the NASA DISCOVER-AQ field campaign in Baltimore/Washington DC and decreases the lifetime of NTR, which improves the CMAQ prediction in organic nitrate and increases NO_x concentration in rural areas (Streets et al. 2013).

- **NO_x prediction change versus O_3 prediction change**

In the atmosphere, O_3 and NO_x concentrations are correlated through chemical reactions. Therefore, the two pivotal questions need asking for further improving O_3 forecasting performance in NAQFC are whether the NO_x bias is related to the O_3 bias and whether reduction in the NO_x bias leads to a reduction in the O_3 bias. Similar to the NO_x diurnal variation (Figure 4d), in the O_3 diurnal variation (Figure 5d), there is also an hourly shift of O_3 concentration at the lowest peak in the morning between the AQS observations and CMAQ simulations. The highest positive bias of O_3 appears at 8 am local time, corresponding to the largest daytime negative biases of NO_x. However, after the NO_x emissions adjustment has been made, the NO_x bias is reduced most at nighttime and the O_3 bias is reduced most during the daytime. During the night, a reduction in NO_x emissions results in a decline in the CMAQ-predicted NO_x concentration, diminishing the NO_x titration effect on ozone. On the other hand, in the New Case, the daytime ozone concentration in CMAQ decreases compared with the Base Case, implying that less ozone remains in the atmosphere after sunset. As a net result, the ozone concentration in CMAQ at night decreases and sequentially the ozone-positive bias at night decreases. During the day, the O_3 bias decreases when the NO_x bias slightly increases, simply because with respect to the

383 CONUS O_3 is sensitive to NO_x and when NO_x emissions reduce, ambient O_3 concentration
384 deceases. To conclude, in this study, although the NO_x bias is shown to be related to the O_3 bias,
385 the reduction in the O_3 bias is not necessarily caused by a decline in the NO_x bias due to the NO_x
386 simulation uncertainties in the inventory and reaction or because of NO_x-related VOC
387 uncertainty such as in its emissions inventory.

388 ## *Conclusions*

389 In this study, NO_x emissions were updated based on an inventory projection. The
390 updated emissions were used in a CMAQ simulation in July 2011 for the evaluation. Overall, the
391 CMAQ-simulated result over the CONUS improves, as shown in the reduction of both the NO_x
392 and O_3 positive biases in the prediction. Although the NO_x bias is related to the O_3 bias, reducing
393 the NO_x bias does not mean a spontaneous O_3 bias reduction because there are remaining
394 problems in the NO_x inventory and CMAQ model configuration.

395 First, the NO_x inventory in regions such as the North East and Rocky Mountains is found
396 to increase instead of following the recent decadal nation-wide trend of decrease in the
397 adjustment according to the satellite observations, ground site measurements and CMAQ model
398 sensitivity simulations. Second, the NO_x inventory in regions such as the Lower Middle has
399 indicated a decrease larger than that the adjustment has determined. Third, the diurnal variability
400 of NO_x illustrates that the NO_x overestimation during the nighttime has decreased but yet
401 increased during the daytime slightly after a new NO_x inventory has been applied to a CMAQ
402 simulation. It is because that not only the NO_x inventory but also physical and chemical
403 mechanisms pertinent to NO_x production and loss as well as meteorology parameters
404 implemented in CMAQ are needed for further investigations.

Acknowledgement

This work is partially funded by the U.S. National Aeronautics and Space Administration (NASA) under the auspices of the Air Quality Applied Science Team (AQAST) program. The authors are thankful to Drs. Armistead G. Russell, Mehmet Talat Odman and Yongtao Hu of the school of Civil and Environmental Engineering, the Georgia Institute of Technology, for the many insightful discussions that richly benefited this work.

411 ## *References:*

412 Appel, K. W., Roselle, S. J., Gilliam, R. C. and Pleim, J. E.: Sensitivity of the Community Multiscale Air
413 Quality (CMAQ) model v4.7 results for the eastern United States to MM5 and WRF
414 meteorological drivers, Geoscientific Model Development, 3(1), 169-188, 2010.
415 Bar-Ilan, A., Grant, J., Parikh, R., Pollack, A., Henderer, D., Pring, D. and Sgamma, K.: Development of
416 Baseline 2006 Emissions from Oil and Gas Activity in the Piceance Basin, Prepared for Western
417 Governor's Association. Prepared by ENVIRON International Corporation, Novato, CA.
418 http://www. wrapair. org/forums/ogwg/documents/2009-
419 01_06_Baseline_Emissions_Piceance_Basin_Technical_Memo_01-20. pdf, 2009.
420 Beaver, M. R., St Clair, J. M., Paulot, F., Spencer, K. M., Crounse, J. D., LaFranchi, B. W., Min, K. E.,
421 Pusede, S. E., Wooldridge, P. J., Schade, G. W., Park, C., Cohen, R. C. and Wennberg, P. O.:
422 Importance of biogenic precursors to the budget of organic nitrates: observations of
423 multifunctional organic nitrates by CIMS and TD-LIF during BEARPEX 2009, Atmospheric
424 Chemistry and Physics, 12(13), 5773-5785, 2012.
425 Bey, I., Jacob, D. J., Logan, J. A. and Yantosca, R. M.: Asian chemical outflow to the Pacific in spring:
426 Origins, pathways, and budgets, Journal of Geophysical Research-Atmospheres, 106(D19),
427 23097-23113, 2001.
428 Bishop, G. A. and Stedman, D. H.: A decade of on-road emissions measurements, Environmental Science
429 & Technology, 42(5), 1651-1656, 2008.
430 Boersma, K. F., Eskes, H. J. and Brinksma, E. J.: Error analysis for tropospheric NO2 retrieval from space,
431 Journal of Geophysical Research-Atmospheres, 109(D4), 2004.
432 Boersma, K. F., Eskes, H. J., Veefkind, J. P., Brinksma, E. J., van der A, R. J., Sneep, M., van den Oord, G. H.
433 J., Levelt, P. F., Stammes, P., Gleason, J. F. and Bucsela, E. J.: Near-real time retrieval of
434 tropospheric NO2 from OMI, Atmospheric Chemistry and Physics, 7(8), 2103-2118, 2007.
435 Browne, E. C., Min, K. E., Wooldridge, P. J., Apel, E., Blake, D. R., Brune, W. H., Cantrell, C. A., Cubison, M.
436 J., Diskin, G. S., Jimenez, J. L., Weinheimer, A. J., Wennberg, P. O., Wisthaler, A. and Cohen, R. C.:
437 Observations of total RONO2 over the boreal forest: NOx sinks and HNO3 sources, Atmospheric
438 Chemistry and Physics, 13(9), 4543-4562, 2013.
439 Byun, D. and Schere, K. L.: Review of the governing equations, computational algorithms, and other
440 components of the models-3 Community Multiscale Air Quality (CMAQ) modeling system,
441 Applied Mechanics Reviews, 59(1-6), 51-77, 2006.
442 Carlton, A. G., Bhave, P. V., Napelenok, S. L., Edney, E. D., Sarwar, G., Pinder, R. W., Pouliot, G. A. and
443 Houyoux, M.: Model Representation of Secondary Organic Aerosol in CMAQv4.7, Environmental
444 Science & Technology, 44(22), 8553-8560, 2010.
445 Chai, T., Kim, H. C., Lee, P., Tong, D., Pan, L., Tang, Y., Huang, J., McQueen, J., Tsidulko, M. and Stajner, I.:
446 Evaluation of the United States National Air Quality Forecast Capability experimental real-time
447 predictions in 2010 using Air Quality System ozone and NO2 measurements, Geoscientific Model
448 Development, 6(5), 1831-1850, 2013.
449 Dallmann, T. R. and Harley, R. A.: Evaluation of mobile source emission trends in the United States,
450 Journal of Geophysical Research-Atmospheres, 115, 2010.
451 Davis, J. M., Bhave, P. V. and Foley, K. M.: Parameterization of N2O5 reaction probabilities on the
452 surface of particles containing ammonium, sulfate, and nitrate, Atmospheric Chemistry and
453 Physics, 8(17), 5295-5311, 2008.
454 DOE (2012). Annual Energy Outlook 2012. DOE Energy Information Agency (EIA). Document No.
455 DOE/EIA-0383(2012). Accessed online Novv 18, 2012 at
456 http://www.eia.gov/forecasts/aeo/pdf/0383(2012).pdf.

Doraiswamy, P., Hogrefe, C., Hao, W., Civerolo, K., Ku, J. Y. and Sistla, G.: A Retrospective Comparison of Model-Based Forecasted PM2.5 Concentrations with Measurements, Journal of the Air & Waste Management Association, 60(11), 1293-1308, 2010.

Dunlea, E. J., Herndon, S. C., Nelson, D. D., Volkamer, R. M., San Martini, F., Sheehy, P. M., Zahniser, M. S., Shorter, J. H., Wormhoudt, J. C., Lamb, B. K., Allwine, E. J., Gaffney, J. S., Marley, N. A., Grutter, M., Marquez, C., Blanco, S., Cardenas, B., Retama, A., Villegas, C. R. R., Kolb, C. E., Molina, L. T. and Molina, M. J.: Evaluation of nitrogen dioxide chemiluminescence monitors in a polluted urban environment, Atmospheric Chemistry and Physics, 7(10), 2691-2704, 2007.

Eder, B., Kang, D. W., Mathur, R., Pleim, J., Yu, S. C., Otte, T. and Pouliot, G.: A performance evaluation of the National Air Quality Forecast Capability for the summer of 2007, Atmospheric Environment, 43(14), 2312-2320, 2009.

Eder, B., Kang, D. W., Mathur, R., Yu, S. C. and Schere, K.: An operational evaluation of the Eta-CMAQ air quality forecast model, Atmospheric Environment, 40(26), 4894-4905, 2006.

Ensberg, J. J., Craven, J. S., Metcalf, A. R., Allan, J. D., Angevine, W. M., Bahreini, R., Brioude, J., Cai, C., Coe, H., de Gouw, J. A., Ellis, R. A., Flynn, J. H., Haman, C. L., Hayes, P. L., Jimenez, J. L., Lefer, B. L., Middlebrook, A. M., Murphy, J. G., Neuman, J. A., Nowak, J. B., Roberts, J. M., Stutz, J., Taylor, J. W., Veres, P. R., Walker, J. M. and Seinfeld, J. H.: Inorganic and black carbon aerosols in the Los Angeles Basin during CalNex, Journal of Geophysical Research-Atmospheres, 118(4), 1777-1803, 2013.

EPA (2011). Technical Support Document (TSD) for the final Transport Rule. Docket ID No. EPA-HQ-OAR-2009-0491 (accessed online Nov 18, 2012 at http://www.epa.gov/airtransport/pdfs/EmissionsInventory.pdf). .

Fast, J. D., Doran, J. C., Shaw, W. J., Coulter, R. L. and Martin, T. J.: The evolution of the boundary layer and its effect on air chemistry in the Phoenix area, Journal of Geophysical Research-Atmospheres, 105(D18), 22833-22848, 2000.

Finlayson-Pitts, B. J., Wingen, L. M., Sumner, A. L., Syomin, D. and Ramazan, K. A.: The heterogeneous hydrolysis of NO2 in laboratory systems and in outdoor and indoor atmospheres: An integrated mechanism, Physical Chemistry Chemical Physics, 5(2), 223-242, 2003.

Frost, G. J., McKeen, S. A., Trainer, M., Ryerson, T. B., Neuman, J. A., Roberts, J. M., Swanson, A., Holloway, J. S., Sueper, D. T., Fortin, T., Parrish, D. D., Fehsenfeld, F. C., Flocke, F., Peckham, S. E., Grell, G. A., Kowal, D., Cartwright, J., Auerbach, N. and Habermann, T.: Effects of changing power plant NO(x) emissions on ozone in the eastern United States: Proof of concept, Journal of Geophysical Research-Atmospheres, 111(D12), 2006.

Gorline, J. L. and Lee, P.: Performance evaluation of NOAA-EPA developmental aerosol forecasts, Environmental Fluid Mechanics, 9(1), 109-120, 2009.

Hilboll, A., Richter, A. and Burrows, J. P.: Long-term changes of tropospheric NO2 over megacities derived from multiple satellite instruments, Atmospheric Chemistry and Physics, 13(8), 4145-4169, 2013.

Houyoux, M. R., Vukovich, J. M., Coats, C. J., Wheeler, N. J. M. and Kasibhatla, P. S.: Emission inventory development and processing for the Seasonal Model for Regional Air Quality (SMRAQ) project, Journal of Geophysical Research-Atmospheres, 105(D7), 9079-9090, 2000.

Janjic, Z. I.: A nonhydrostatic model based on a new approach, Meteorology and Atmospheric Physics, 82(1-4), 271-285, 2003.

Kang, D. W., Mathur, R. and Rao, S. T.: Real-time bias-adjusted O-3 and PM2.5 air quality index forecasts and their performance evaluations over the continental United States, Atmospheric Environment, 44(18), 2203-2212, 2010.

Kim, H., Ngan, F., Lee, P., & Tong, D. Development of IDL-based geospatial data processing framework for meteorology and air quality modeling, final report in preparation, 2013.

Kim, S. W., Heckel, A., Frost, G. J., Richter, A., Gleason, J., Burrows, J. P., McKeen, S., Hsie, E. Y., Granier, C. and Trainer, M.: NO2 columns in the western United States observed from space and simulated by a regional chemistry model and their implications for NOx emissions, Journal of Geophysical Research-Atmospheres, 114, 2009.

Kim, S. W., Heckel, A., McKeen, S. A., Frost, G. J., Hsie, E. Y., Trainer, M. K., Richter, A., Burrows, J. P., Peckham, S. E. and Grell, G. A.: Satellite-observed US power plant NO(x) emission reductions and their impact on air quality, Geophysical Research Letters, 33(22), 2006.

Kleinman, L. I., Daum, P. H., Lee, Y. N., Nunnermacker, L. J., Springston, S. R., Weinstein-Lloyd, J. and Rudolph, J.: A comparative study of ozone production in five U.S. metropolitan areas, Journal of Geophysical Research-Atmospheres, 110(D2), 2005.

Lamsal, L. N., Martin, R. V., Padmanabhan, A., van Donkelaar, A., Zhang, Q., Sioris, C. E., Chance, K., Kurosu, T. P. and Newchurch, M. J.: Application of satellite observations for timely updates to global anthropogenic NOx emission inventories, Geophysical Research Letters, 38, 2011.

Lamsal, L. N., Martin, R. V., van Donkelaar, A., Steinbacher, M., Celarier, E. A., Bucsela, E., Dunlea, E. J. and Pinto, J. P.: Ground-level nitrogen dioxide concentrations inferred from the satellite-borne Ozone Monitoring Instrument, Journal of Geophysical Research-Atmospheres, 113(D16), 2008.

Lee, D. S., Kohler, I., Grobler, E., Rohrer, F., Sausen, R., GallardoKlenner, L., Olivier, J. G. J., Dentener, F. J. and Bouwman, A. F.: Estimations of global NOx emissions and their uncertainties, Atmospheric Environment, 31(12), 1735-1749, 1997.

Lee, P., Byun, D., Stein, A., Tang, Y. H., Lin, H. M., Huang, H. C., Lu, S., Tsidulko, M., McQueen, J., Tong, D., Yu, S. C., Chai, T. F., Kim, D., Stajner, I. and Davidson, P. (2010). Effect of Temporal Averaging of Vertical Eddy Diffusivity on the Forecast Quality of Surface Ozone Concentration of the National Air Quality Forecast. Air Pollution Modeling and Its Application Xx. D. G. Steyn and S. T. Rao**:** 295-301.

Lee, P., Tang, Y. H., Kang, D. W., McQueen, J., Tsidulko, M., Huang, H. C., Lu, S., Hart, M., Lin, H. M., Yu, S. C., DiMego, G., Stajner, I. and Davidson, P.: Impact of consistent boundary layer mixing approaches between NAM and CMAQ, Environmental Fluid Mechanics, 9(1), 23-42, 2009.

Lei, W. F., Zhang, R. Y., Tie, X. X. and Hess, P.: Chemical characterization of ozone formation in the Houston-Galveston area: A chemical transport model study, Journal of Geophysical Research-Atmospheres, 109(D12), 2004.

Lin, J. T., Youn, D., Liang, X. Z. and Wuebbles, D. J.: Global model simulation of summertime US ozone diurnal cycle and its sensitivity to PBL mixing, spatial resolution, and emissions, Atmospheric Environment, 42(36), 8470-8483, 2008.

Lindhjem, C. E., Pollack, A. K., DenBleyker, A. and Shaw, S. L.: Effects of improved spatial and temporal modeling of on-road vehicle emissions, Journal of the Air & Waste Management Association, 62(4), 471-484, 2012.

Liu, P., Zhang, Y., Yu, S. and Schere, K. L.: Use of a process analysis tool for diagnostic study on fine particulate matter predictions in the U.S. - Part II: Analyses and sensitivity simulations, Atmospheric Pollution Research, 2(1), 61-71, 2011.

Marr, L. C., Black, D. R. and Harley, R. A.: Formation of photochemical air pollution in central California - 1. Development of a revised motor vehicle emission inventory, Journal of Geophysical Research-Atmospheres, 107(D5-6), 2002.

McDonald, B. C., Dallmann, T. R., Martin, E. W. and Harley, R. A.: Long-term trends in nitrogen oxide emissions from motor vehicles at national, state, and air basin scales, Journal of Geophysical Research-Atmospheres, 117, 2012.

Murphy, C. F. and Allen, D. T.: Hydrocarbon emissions from industrial release events in the Houston-Galveston area and their impact on ozone formation, Atmospheric Environment, 39(21), 3785-3798, 2005.

Otte, T. L., Pouliot, G., Pleim, J. E., Young, J. O., Schere, K. L., Wong, D. C., Lee, P. C. S., Tsidulko, M., McQueen, J. T., Davidson, P., Mathur, R., Chuang, H. Y., DiMego, G. and Seaman, N. L.: Linking the Eta Model with the Community Multiscale Air Quality (CMAQ) modeling system to build a national air quality forecasting system, Weather and Forecasting, 20(3), 367-384, 2005.

Perring, A. E., Bertram, T. H., Wooldridge, P. J., Fried, A., Heikes, B. G., Dibb, J., Crounse, J. D., Wennberg, P. O., Blake, N. J., Blake, D. R., Brune, W. H., Singh, H. B. and Cohen, R. C.: Airborne observations of total RONO2: new constraints on the yield and lifetime of isoprene nitrates, Atmospheric Chemistry and Physics, 9(4), 1451-1463, 2009.

Phillips, S. B. and Finkelstein, P. L.: Comparison of spatial patterns of pollutant distribution with CMAQ predictions, Atmospheric Environment, 40(26), 4999-5009, 2006.

Richter, A., Begoin, M., Hilboll, A. and Burrows, J. P.: An improved NO2 retrieval for the GOME-2 satellite instrument, Atmospheric Measurement Techniques, 4(6), 1147-1159, 2011.

Russell, A. R., Valin, L. C., Bucsela, E. J., Wenig, M. O. and Cohen, R. C.: Space-based Constraints on Spatial and Temporal Patterns of NOx Emissions in California, 2005-2008, Environmental Science & Technology, 44(9), 3608-3615, 2010.

Sarwar, G., Roselle, S. J., Mathur, R., Appel, W., Dennis, R. L. and Vogel, B.: A comparison of CMAQ HONO predictions with observations from the northeast oxidant and particle study, Atmospheric Environment, 42(23), 5760-5770, 2008.

Sillman, S.: The relation between ozone, NOx and hydrocarbons in urban and polluted rural environments, Atmospheric Environment, 33(12), 1821-1845, 1999.

Stavrakou, T., Muller, J. F., Boersma, K. F., De Smedt, I. and van der A, R. J.: Assessing the distribution and growth rates of NO(x) emission sources by inverting a 10-year record of NO(2) satellite columns, Geophysical Research Letters, 35(10), 2008.

Streets, D. G., Canty, T., Carmichael, G. R., de Foy, B., Dickerson, R. R., Duncan, B. N., Edwards, D. P., Haynes, J. A., Henze, D. K., Houyoux, M. R., Jacobi, D. J., Krotkov, N. A., Lamsal, L. N., Liu, Y., Lu, Z. F., Martini, R. V., Pfister, G. G., Pinder, R. W., Salawitch, R. J. and Wechti, K. J.: Emissions estimation from satellite retrievals: A review of current capability, Atmospheric Environment, 77, 1011-1042, 2013.

Valks, P., Pinardi, G., Richter, A., Lambert, J. C., Hao, N., Loyola, D., Van Roozendael, M. and Emmadi, S.: Operational total and tropospheric NO2 column retrieval for GOME-2, Atmospheric Measurement Techniques, 4(7), 1491-1514, 2011.

van der A, R. J., Peters, D., Eskes, H., Boersma, K. F., Van Roozendael, M., De Smedt, I. and Kelder, H. M.: Detection of the trend and seasonal variation in tropospheric NO2 over China, Journal of Geophysical Research-Atmospheres, 111(D12), 2006.

Velders, G. J. M., Granier, C., Portmann, R. W., Pfeilsticker, K., Wenig, M., Wagner, T., Platt, U., Richter, A. and Burrows, J. P.: Global tropospheric NO(2) column distributions: Comparing three-dimensional model calculations with GOME measurements, Journal of Geophysical Research-Atmospheres, 106(D12), 12643-12660, 2001.

Wilczak, J. M., Djalalova, I., McKeen, S., Bianco, L., Bao, J. W., Grell, G., Peckham, S., Mathur, R., McQueen, J. and Lee, P.: Analysis of regional meteorology and surface ozone during the TexAQS II field program and an evaluation of the NMM-CMAQ and WRF-Chem air quality models, Journal of Geophysical Research-Atmospheres, 114, 2009.

595 Xing, J., Pleim, J., Mathur, R., Pouliot, G., Hogrefe, C., Gan, C. M. and Wei, C.: Historical gaseous and
596 primary aerosol emissions in the United States from 1990 to 2010, Atmospheric Chemistry and
597 Physics, 13(15), 7531-7549, 2013.
598 Yarwood, G., Rao, S., Yocke, M. and Whitten, G. Z. (2005). Updates to the Carbon Bond chemical
599 mechanism: CB05. Final Report to the US EPA, RT-0400675, December 8, 2005,
600 http://www.camx.com/publ/pdfs/CB05_Final_Report_120805.pdf.

601

602

Tables:

Table 1, NO_x emissions inventories used in the two scenarios: Base Case and New Case

Source		Base	New
Mobile		2005 MOBILE6	2005 MOBILE6 + 05 to 12 Projections (EPA 2011)
Point Sources		NEI05v1	2010 CEM + DOE Annual Energy Outlook (DOE 2012)
Area Source	Non-Road	NEI05v1	CSAPR (EPA 2011)
	Other Sectors	NEI05v1	NEI05v1
Biogenic Emissions		BEIS3.13 (CMAQ 4.7.1 inline)	BEIS3.13 (CMAQ 4.7.1 inline)
Canadian Emissions		2001 EI	2006 EI

Table 2, The CONUS-wide emissions reductions under various categories in July 2011

	weekday	**weekend**	**weekly**
area	-10.5%	-3.6%	-8.1%
mobile	-37.8%	-37.9%	-37.8%
point	-4.2%	-4.0%	-4.1%
Total	-18.3%	-13.5%	-17.2%
surface	-23.9%	-18.6%	-22.2%

Table 3, NO_x and O_3 biases (ppbv) over the CONUS according to the three land-use types: urban, suburban and rural.

Land Use	NO_x_Bias[1]		ΔNO_x	O_3_Bias[2]		ΔO_3
	Base	New	(New-Base)	Base	New	(New-Base)
Urban	2.80	0.46	-2.34	7.08	6.16	-0.92
Suburban	4.62	2.53	-2.09	7.48	6.22	-1.26
Rural	0.75	0.18	-0.57	7.80	5.93	-1.87

[1]: The total NO_x AQS sites are 295 including urban (101), suburban (111) and rural (83).

[2]: The total O_3 AQS sites are 1144 including urban (201), suburban (438) and rural (505).

Figures:

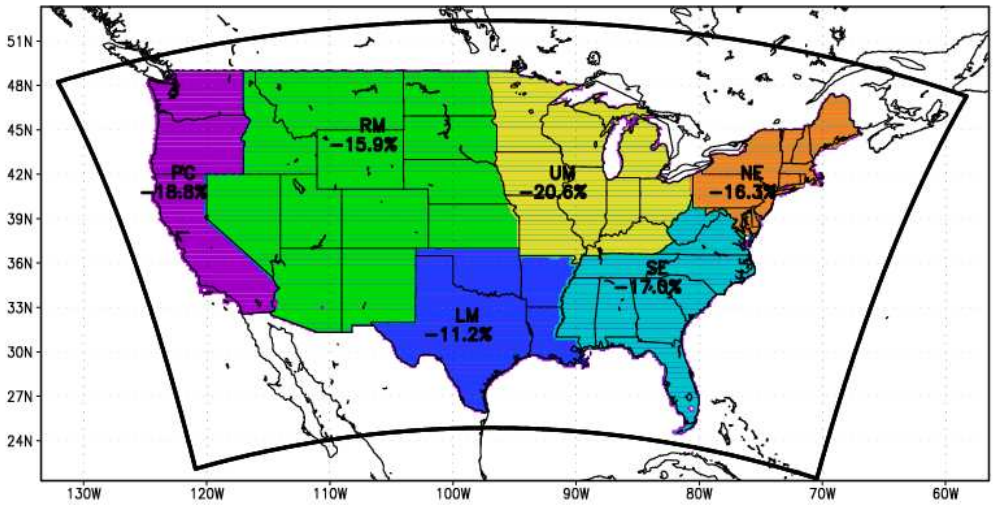

Figure 1, NAQFC-β system simulation domain (442×265) and six predefined geographic regions in the CONUS: Pacific Coast (PC), Rocky Mountains (RM), Lower Middle (LM), Upper Middle (UM), South East (SE) and North East (NE). The horizontal grid resolution is 12 km. The bold dark line represents the outer perimeter of the CONUS computational domain. The number in each region represents the percentage of NO_x emissions changes due to the NO_x emissions inventory adjustment schemes in this study.

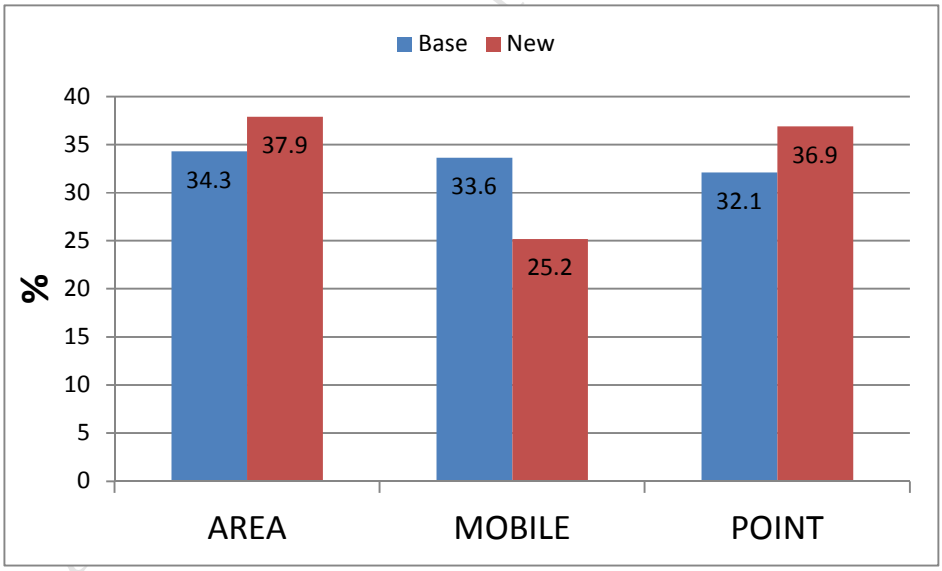

Figure 2, the percentage contribution to total anthropogenic NO_x emissions from the three NO_x emissions sectors before and after the application of the adjustment schemes.

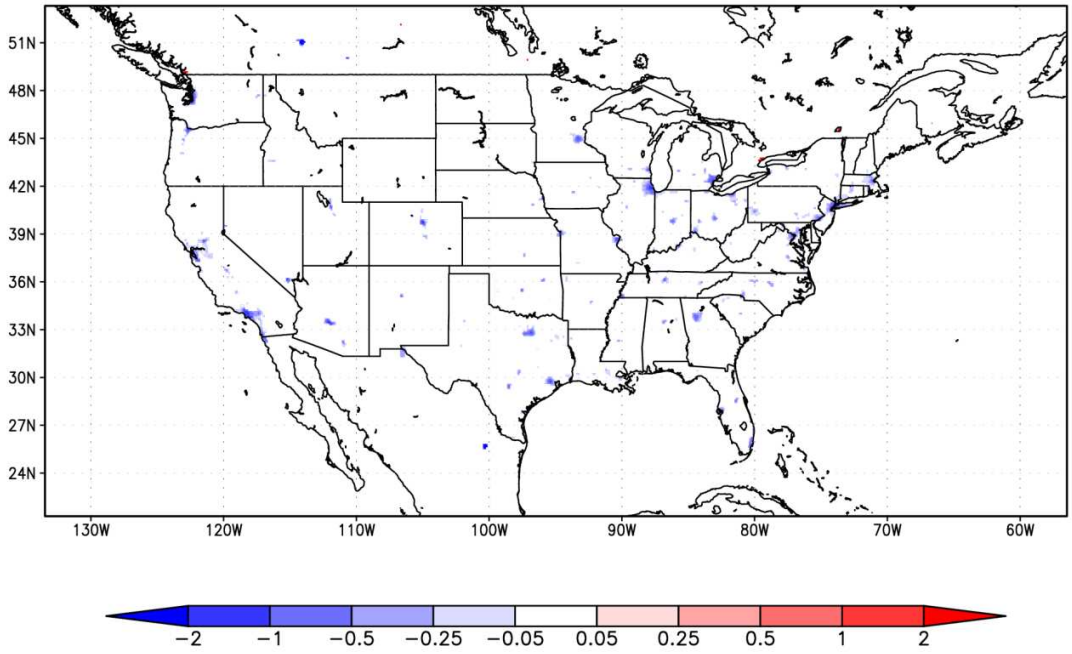

Figure 3a, CMAQ NO_x emissions flux differences (moles sec^{-1} $grid^{-1}$) between the Base Case and New Case (New – Base).

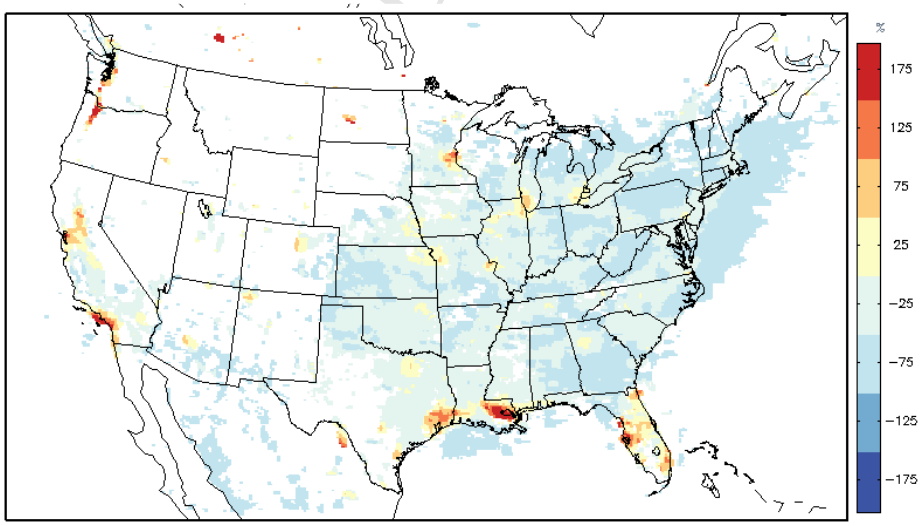

Figure 3b, (CMAQ-GOME-2)/GOME-2 NO_2 ratio in July 2011

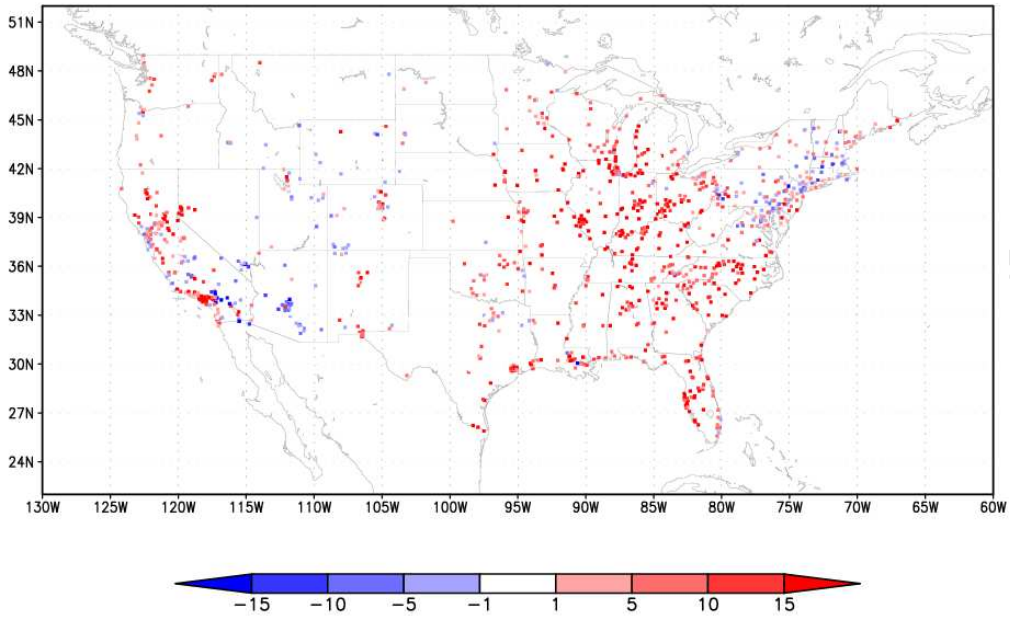

Figure 4a, NO_x monthly averaged bias (ppbv) in the Base Case based on verification with the AQS data (295 sites) for July 2011.

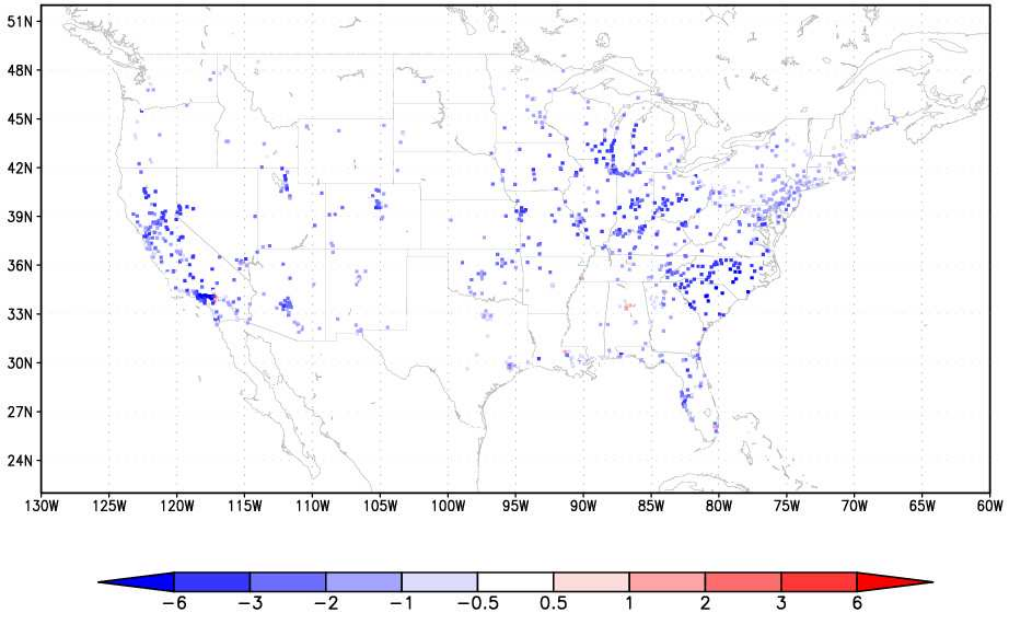

Figure 4b, Simulated NO_x concentration differences (ppbv) between the New Case and Base Case (New – Base) in July 2011.

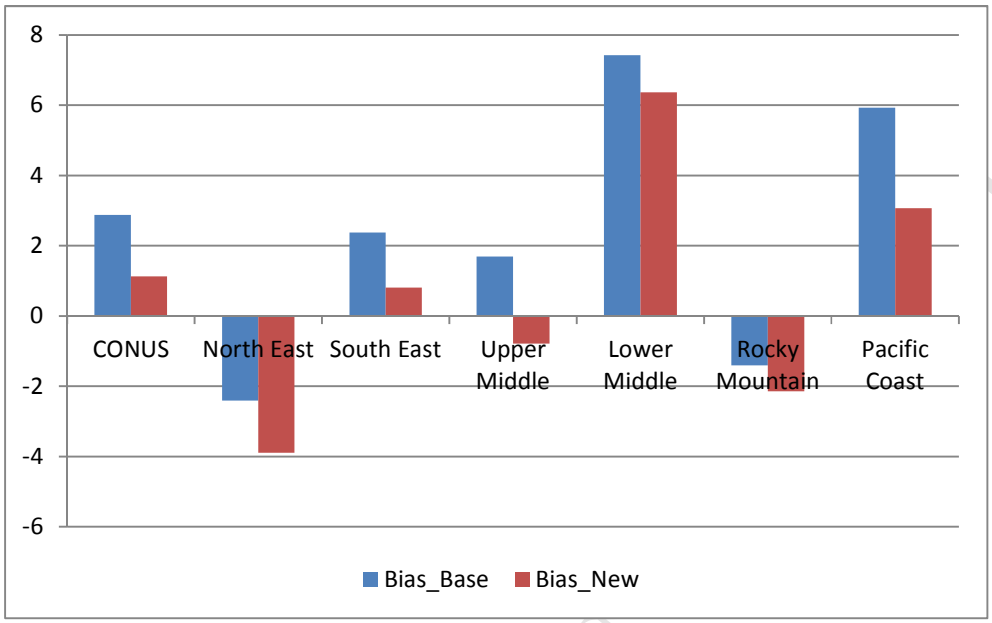

Figure 4c, NO_x bias (ppbv) in the six predefined regions.

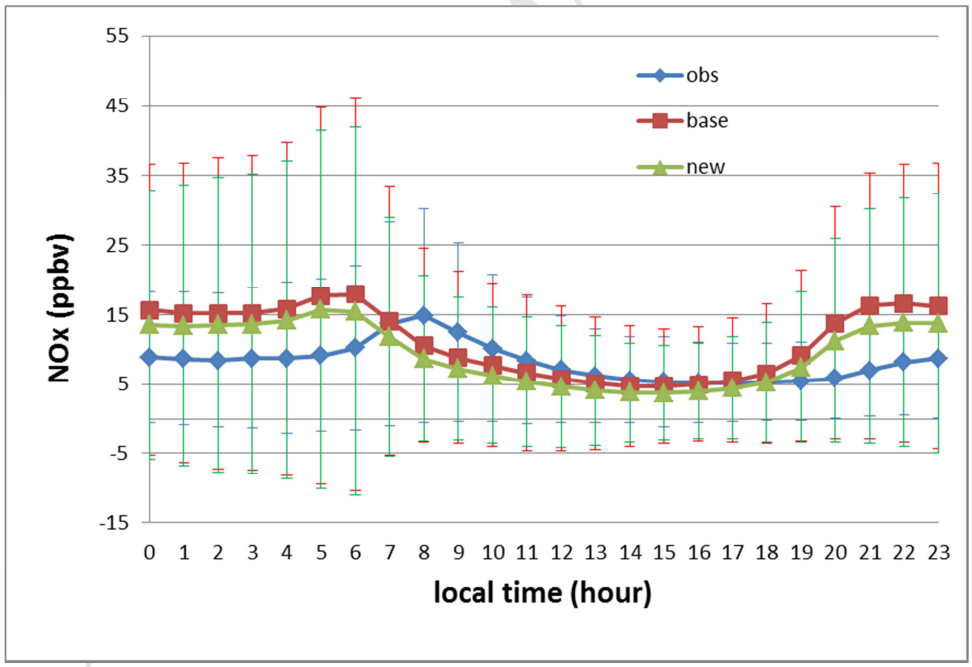

Figure 4d, Diurnal NO_x variations in the AQS and model simulations in July 2011. The error bars represent NO_x standard deviation.

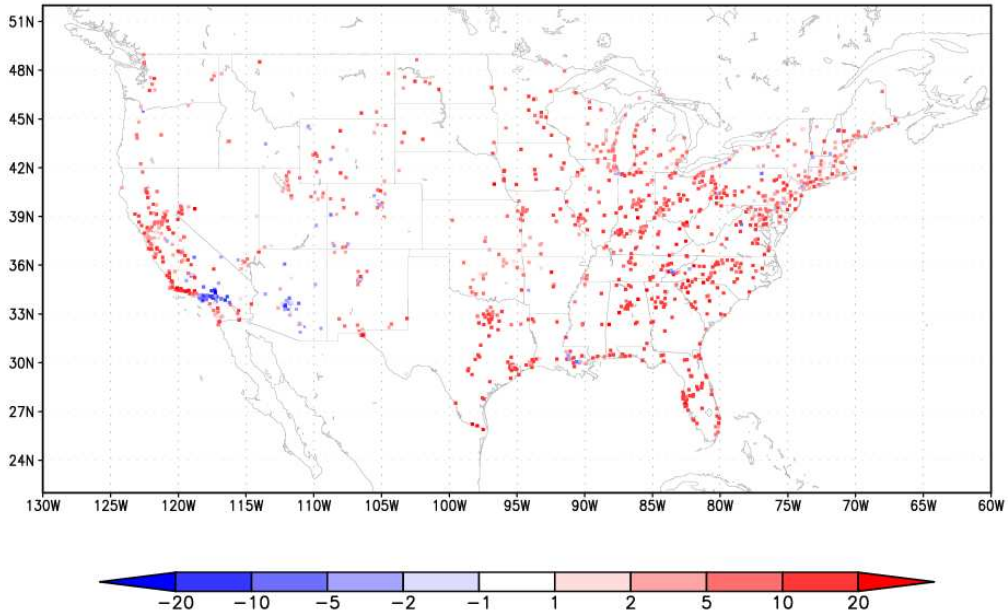

Figure 5a, O_3 monthly averaged bias (ppbv) in the Base Case based on verification with the AQS data (1144 sites) for July 2011.

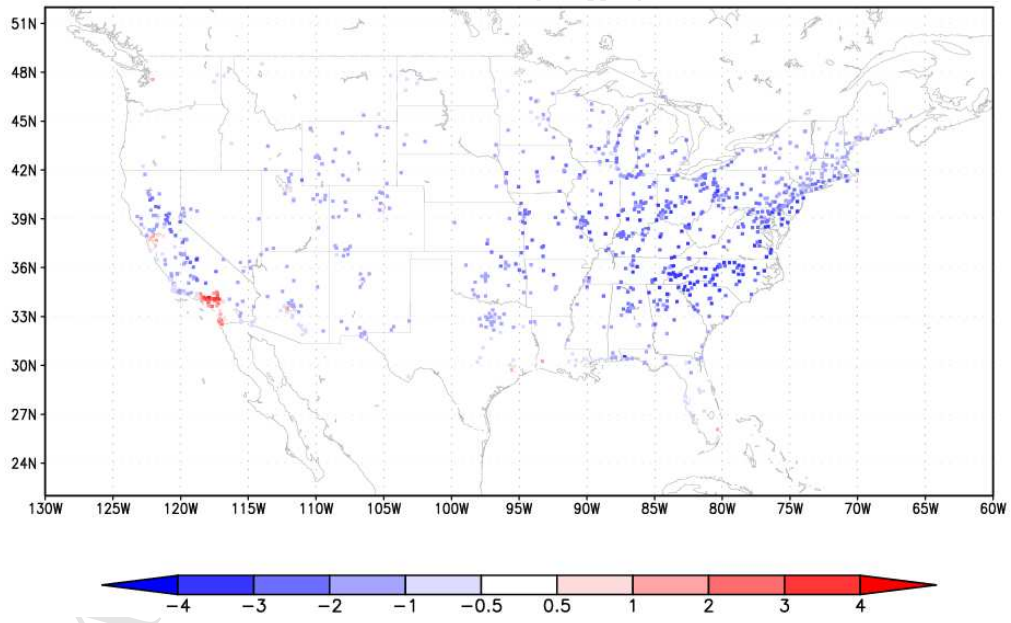

Figure 5b, Simulated O_3 concentration differences (ppbv) between the New Case and Base Case (New – Base) in July 2011.

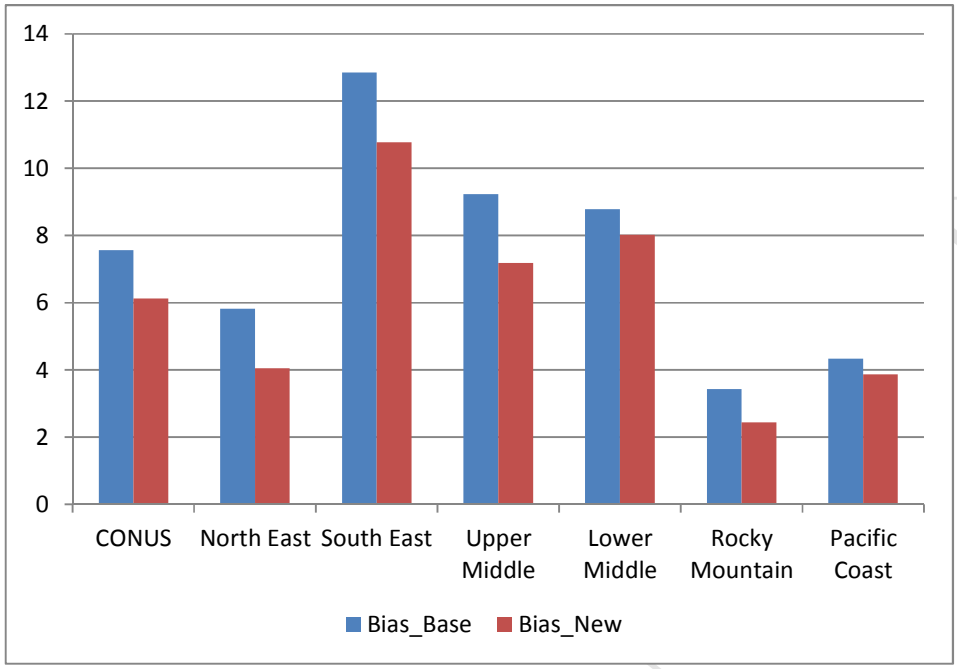

Figure 5c, O_3 bias (ppbv) in the Base Case and New Case for the six predefined regions.

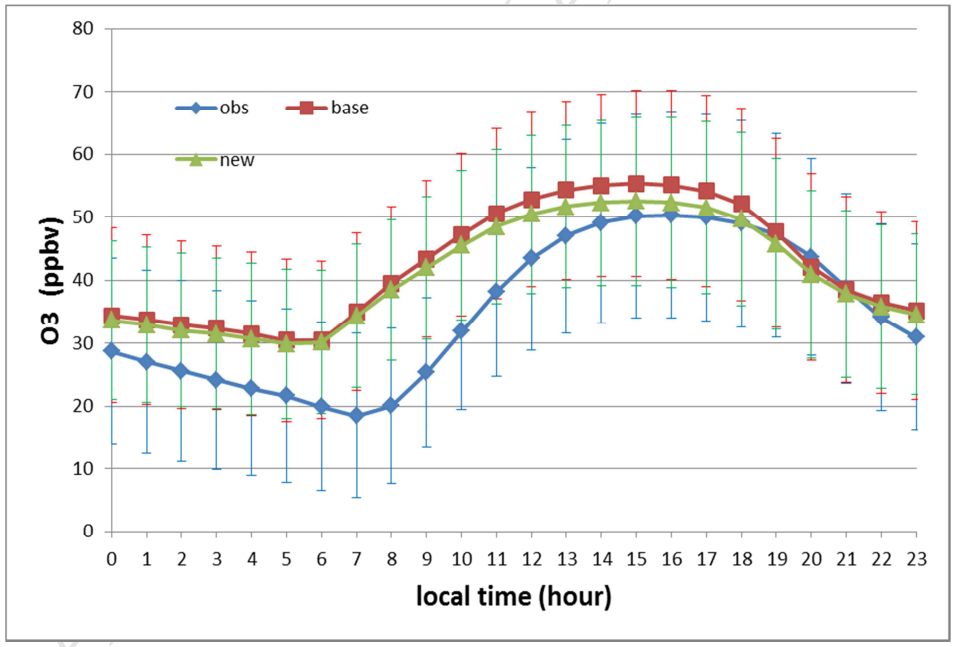

Figure 5d, Diurnal O_3 variations in AQS and model simulations in July 2011. The error bars represent O_3 standard deviation.